

Estimating Gait Speed in the Real World With a Head-Worn Inertial Sensor

Original

Estimating Gait Speed in the Real World With a Head-Worn Inertial Sensor / Tasca, P., Salis, F., Rosati, S., Balestra, G., Mazza, C., Cereatti, A.. - In: IEEE TRANSACTIONS ON NEURAL SYSTEMS AND REHABILITATION ENGINEERING. - ISSN 1534-4320. - ELETTRONICO. - 33:(2025), pp. 858-867. [10.1109/TNSRE.2025.3542568]

Availability:

This version is available at: 11583/2999424 since: 2025-04-22T10:06:13Z

Publisher:

IEEE

Published

DOI:10.1109/TNSRE.2025.3542568

Terms of use:

This article is made available under terms and conditions as specified in the corresponding bibliographic description in the repository

Publisher copyright

(Article begins on next page)

Estimating Gait Speed in the Real World With a Head-Worn Inertial Sensor

Paolo Tasca¹, Francesca Salis², Samanta Rosati³, *Member, IEEE*, Gabriella Balestra⁴, *Member, IEEE*, Claudia Mazzà⁵, and Andrea Cereatti⁶, *Member, IEEE*

Abstract—Head-worn inertial sensors represent a valuable option to characterize gait in real-world conditions, thanks to the integration with glasses and hearing aids. Few methods based on head-worn sensors allow for stride-by-stride gait speed estimation, but none has been developed with data collected in real-world settings. This study aimed at validating a two-steps machine learning method to estimate initial contacts and stride-by-stride speed in real-world gait using a single inertial sensor attached to the temporal region. A convolutional network is used to detect strides. Then, stride-by-stride gait speed is inferred from the detected cycles by a gaussian process regression model. A multi-sensor wearable system was used to label over 100,000 strides recorded from 15 healthy young adults during supervised acquisitions and real-world unsupervised walking. The stride detector achieved high detection rate (F1-score > 92%) and accuracy (mean absolute error < 40 ms). Very strong correlation between target and predicted speed (Spearman coefficient > 0.86) and low mean absolute error (< 0.085 m/s) were observed. The method proved valid for the quantitative evaluation of stride-by-stride gait speed in real-world conditions. These findings lay the technical and analytical groundwork for future clinical validation and application of gait analysis frameworks that integrate inertial sensors with head-worn devices.

Index Terms—Gait speed, head-worn IMU, machine learning, unsupervised walking, wearable sensors.

I. INTRODUCTION

REAL world gait, and gait speed in particular, are highly targeted measures both in health- and disease-related applications [1], [2]. These can be continuously collected with wearable inertial measurement units (IMU) [3]. While IMU dedicated to this endeavor are typically worn on the

wrist [4], [5], [6], lower limbs [7], [8], or trunk [9], [10], [11], recent advances in optical or audiology devices represent a promising solution to reduce users' burden while increasing potential of gathering high density data [12], [13]. To achieve this goal, however, robust algorithms based on data collected from the head in unconstrained real-world scenarios are needed. Several methods to estimate gait spatio-temporal parameters with head-worn IMU (H-IMU) were validated in both healthy [14], [15], [16], [17], [18], [19], [20], [21], [22] and pathological cohorts [23], [24], [25], [26], reporting errors from 0.3 to 4% for temporal parameters and from 6 to 15% for spatial parameters. Yet, none were validated against real-world data i.e., data collected in unsupervised free-living conditions, which present greater complexity and variability compared to controlled laboratory settings [27].

Existing approaches for gait speed estimation often utilize fixed-time windows [28], [29]. However, stride-by-stride parameters might improve the estimation of the gait parameters of interest, provide additional insights into aspects such as gait variability [30], and allow for further applications, such as those involving real-time feedback [31] and robotic control [32]. For the estimation of gait speed on a stride basis, strides have to be preliminarily segmented by detecting stride-related gait events, such as initial contacts (ICs) [33]. These can be detected by exploiting signal heuristics i.e., peaks or zero-crossings of the angular rate and/or acceleration signals along specific axes [34]. Then, gait speed is typically calculated by combining the temporal information derived from the IC timings (e.g., stride duration, cadence) with the spatial information derived from acceleration (e.g., stride length) [35]. Although this approach proved valid in laboratory settings, the uncertainty of the sensor-to-segment alignment in unsupervised conditions and the added complexity of real-world gait signals caused by activity levels and environmental contexts often limit its applicability outside controlled environments [8]. Previous studies showed that machine learning methods can outperform traditional approaches in these scenarios, providing a strong rationale for their use in real-world gait analysis applications [36]. The aim of this study is to assess the ecological validity of a method based on a H-IMU and machine learning in the estimation of stride-by-stride gait speed in real-world conditions. The main contributions of this study are the development of a method for stride-by-stride gait speed estimation with data of a head-worn

Received 11 July 2024; revised 10 January 2025; accepted 4 February 2025. Date of publication 14 February 2025; date of current version 26 February 2025. (*Corresponding author: Paolo Tasca.*)

This work involved human subjects in its research. Approval of all ethical and experimental procedures and protocols was granted by the University Hospital of Cagliari under Approval No. PG/2021/1195.

Paolo Tasca, Samanta Rosati, Gabriella Balestra, and Andrea Cereatti are with the Department of Electronics and Telecommunications, Politecnico di Torino, 10129 Turin, Italy (e-mail: paolo.tasca@polito.it; samanta.rosati@polito.it; gabriella.balestra@polito.it; andrea.cereatti@polito.it).

Francesca Salis was with the Department of Biomedical Sciences, University of Sassari, 07100 Sassari, Italy. She is now with SynDiag s.r.l., 10129 Turin, Italy (e-mail: fsalis1@uniss.it).

Claudia Mazzà is with INDIVI, 4051 Basel, Switzerland (e-mail: claudia.mazza@indivi.io).

Digital Object Identifier 10.1109/TNSRE.2025.3542568

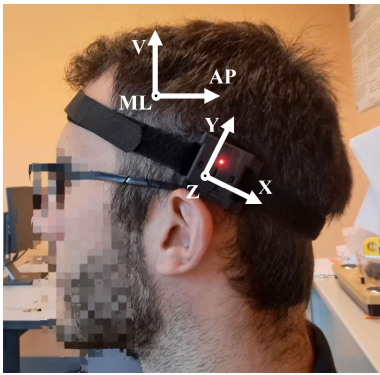


Fig. 1. The H-IMU frame (x, y, z) was roughly aligned to a coordinate system based on the main anatomical axes: ML (medial-to-lateral), V (vertical), and AP (posterior-to-anterior).

IMU. The novelty of the work lies in its validation against a multi-sensor wearable reference system under real-world walking conditions, including both indoor and outdoor walking during daily-life activities.

II. METHODS

A. Experimental Protocol and Setup

Fifteen healthy participants (7 females and 8 males; from 21 to 30 years old) were recruited for the study after providing written informed consent. The number of participants was determined as a trade-off between the rapidity of data collection and processing, and the need to gather a sufficient number of strides to train robust machine learning algorithms (see Section II-B) [37]. Each participant performed two acquisition sessions. First, subjects were asked to walk straight along a 12-meter corridor at three self-selected speeds, and at comfortable speed around a 24-meter oval walk path. Each trial was repeated thrice (*Lab-Based* dataset). Then, subjects underwent a 2.5-hour acquisition period in the real world with no supervision (*Real-World* dataset). During this session, participants were asked to engage in their usual activities with no specific restrictions [11]. The purpose of this acquisition was to introduce walking factors that are hardly reproducible in structured settings, such as fast turns, distractors (e.g., sounds, signs), or obstacles (e.g., cars, other people). Subjects were equipped with the INertial module with DIstance sensors and Pressure insoles (INDIP) system [38]. The INDIP system is a wearable multi-sensor system for motion analysis that incorporates piezo-resistive pressure insoles, magneto IMU and time-of-flight distance sensors. The INDIP system has been extensively validated for daily life use [38], and adopted as reference system for real-world gait in a number of studies [4], [8], [9], [10], [11], [39]. The adopted configuration included three magneto IMU (feet and lower back) and two pressure insoles. One additional IMU was fixed on the left temporal region of the head (H-IMU), a common positioning site for head-worn inertial sensors [40] (Fig. 1). All sensors sampled at 100 Hz. The experimental protocol conformed with the Declaration of Helsinki and was reviewed and approved by the Ethics Committee of the University Hospital of Cagliari (Prot. PG/2021/1195).

B. Data Preparation

First, level gait sequences including at least two left and two right strides, referred to as *walking bouts* (WBs), were segmented using a validated gait sequence detection algorithm based on the INDIP system [38]. Acceleration and angular velocity recorded by the H-IMU during WBs were used as inputs to the method (predictors), while the INDIP system generated the *target ICs* and *target gait speed* through a validated algorithm [38]. The Real-World dataset consisted of over 2200 minutes of data, including almost 1000 WBs. The WBs of all participants accounted for more than 100.000 strides, a reasonably high number of instances to describe gait characteristics, compared to similar studies [41], [42]. Real-world gait exhibited greater complexity than walking in structured settings. This was reflected by WBs duration: one third of the Real-World dataset included WBs shorter than 10s, which may be associated to movements in confined indoor spaces such as the home environment [9]. WBs duration of Real-World data also showed greater variability (coefficient of variation: 1.91) compared to Lab-Based data (coefficient of variation: 0.16). In addition, the distribution of range of motion values showed consistently greater variability and median values for Real-World WBs (roll: 28.8° , yaw: 68.7° , pitch: 43.0°) compared to Lab-Based WBs (roll: 12.4° , yaw: 16.0° , pitch: 19.6°). Gait speed values as measured by the INDIP system ranged from 0.12 m/s to 2 m/s, covering the whole needed range of speeds for the analysis.

Once the WBs were detected by the INDIP system, data from ten participants were randomly assigned to a *construction set* (774 Real-World WBs, 120 Lab-Based WBs, 77821 strides), while data of the remaining five constituted the *test set* (380 Real-World WBs, 60 Lab-Based WBs, 27498 strides), which were not used at training. Participants, and consistently all of their WBs, were assigned randomly after verifying that the target variable (gait speed) was similarly distributed across all participants. The data preparation steps were performed with the licensed software Matlab (v. 2022a, The Mathworks Inc., Natick, MA, USA). Recorded data is available at <https://iee-dataport.org/documents/towalk>.

C. Method Overview

At inference, the method was fed with acceleration and angular velocity (predictors) recorded by the H-IMU during an input WB. Typical gait-related fluctuations in head inertial signals are associated to frequencies lower than 5 Hz [21], [43], [44]. Therefore, predictors were filtered upstream of each block with a 10th order Butterworth low-pass filter with 5 Hz cut-off frequency. The method included two main blocks (Fig. 2):

- 1) *Stride detector*: Detects the time steps at which ICs occur within the input WB and uses them to identify the strides within it. It returns the predicted ICs in the input WB.
- 2) *Gait speed estimator*: Calculates features on a stride-to-stride basis and processes them to estimate gait speed. It returns predicted stride-to-stride gait speed values.

To limit error propagation, the two blocks were trained separately i.e., features fed to the gait speed estimator were derived

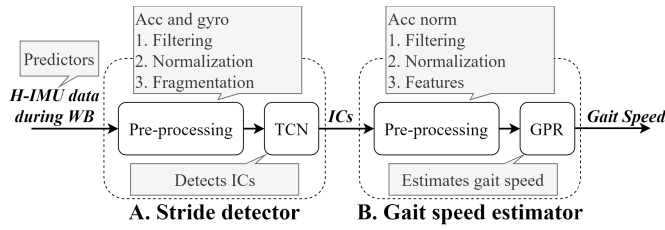


Fig. 2. Overview of the method for ICs and gait speed estimation. Acc: acceleration; gyro: angular velocity.

from strides segmented by the INDIP system. Code examples are available at <https://github.com/H-MOVE-LAB/headgait>.

D. Step 1 - Stride Detector

Previous methods for ICs detection were developed on heuristics under controlled conditions and their applicability to real-world gait might be critical [8]. Generalization of these methods under real-world conditions is expected to be even more problematic when IMU are fixed to body segments whose movement is not directly related to gait progression (e.g., head, wrists) [4]. Machine learning algorithms can overcome such limitation by detecting gait events directly from ecological labeled data rather than relying on heuristic rules derived from specific experimental observations. For example, Hidden Markov models [45], support vector machines [46], decision trees [47], and neural networks [48] were proposed to detect gait events. In contrast to traditional machine learning, the deep learning approach is less demanding in terms of handcrafting of features and required model assumptions (e.g., the number of states for Hidden Markov models), allowing greater versatility with respect to shallow machine learning models [37]. Recently, convolutional neural networks were successfully applied to ICs detection with foot-mounted IMU in structured [22], [39] and real-world settings [8].

In the present study, a similar architecture is proposed to detect ICs and segment strides from data recorded by a single H-IMU. The algorithm was developed using the Python library Keras.

1) *Preprocessing*: Predictors were filtered and scaled by their mean and standard deviation (SD) in each WB and fragmented into equal-length windows of size N ($N = 200$ data points) with a 50% overlap to get one prediction per second.

2) Temporal Convolutional Network:

a) *Architecture*: ICs were detected by a deep learning model trained to return an output sequence (the IC likelihood) given a predictors' input sequence. The model consisted in a Temporal Convolutional Network (TCN) [49] with a 1D-fully connected architecture [50] followed by a fully connected dense layer. The TCN performed non-causal convolutions between layers and 1D filters (kernels). Convolutions were dilated by an exponentially increasing dilation factor to increase the size of the receptive field of the network and recruit information about remote time instants [51]. The TCN featured with residual blocks (Fig. 3). Every residual block included two sequences containing a dilated 1D convolutional layer [52], a batch normalization layer [53], a rectified linear unit (ReLU) activation layer, and a spatial dropout layer [54].

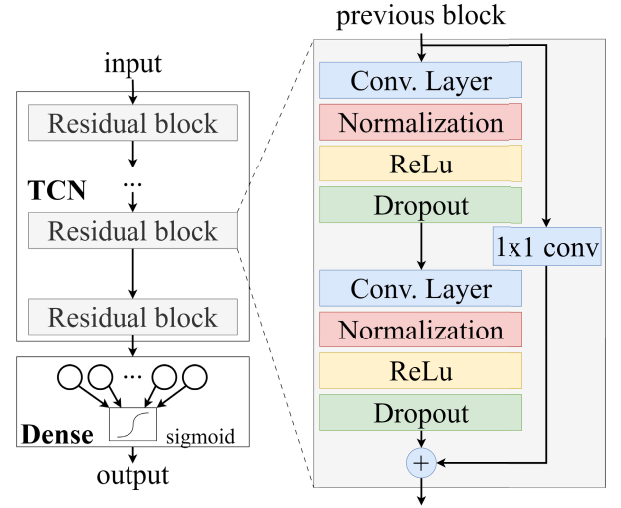


Fig. 3. The architecture of the deep learning model for ICs detection. A 1×1 convolution of the input array (i.e., convolution with a scalar) was optionally performed to ensure that elementwise addition received compatible arrays [51].

TABLE I
GRID SEARCH SPACE FOR HYPERPARAMETERS TUNING

| Hyperparameter | Possible values |
|-------------------|--|
| Number of filters | 4; 8; 16; 32; 64 ; 128; 256 |
| Kernel size | 3; 5; 7; 9 |
| Dilations | [1, 2]; [1, 2, 4]; [1, 2, 4, 8]; [1, 2, 4, 8, 16]; [1, 2, 4, 8, 16, 32] ; [1, 2, 4, 8, 16, 32, 64] |

Optimal hyperparameter values are reported in bold.

A residual connection was used to add the convoluted input to the input of the residual block [55]. The array returned by the TCN layer was fed to a dense layer with sigmoidal activation that returned the IC likelihood in the range [0,1].

b) *Training*: Target ICs were used to label the predictors. Specifically, a predictor array (of size $6 \times N$) and its corresponding label (of size $1 \times N$) constituted an instance. The TCN was trained with the instances of the construction set, divided into a *training set* (data of nine participants) and a *validation set* (data of the remaining participant). Instances of the training set were used to train the network, while instances of the validation set were used to compute the validation loss over training epochs and prevent overfitting. Since the number of non-IC points in an instance was from 50 to 100 times greater than that of ICs, a weighted mean squared error (wMSE) was adopted as loss function to compensate for the unbalance (1):

$$wMSE = \left(\frac{1}{ND} \sum_{i=1}^{ND} y_i - \hat{y}_i \right) \left(\frac{1}{ND} \sum_{i=1}^{ND} y_i + \alpha \right) \quad (1)$$

where N is size of the input window ($N = 200$), D is the batch size ($D = 16$), α is a weighting factor ($\alpha = 0.003$), and \hat{y} and y are the predicted and target responses for a training batch.

c) *Hyperparameters tuning*: To select the optimal architecture, the number of kernels, the kernel size, and the dilation factors were optimized with a grid search strategy (Table I). For robustness, a leave-one-participant-out protocol was adopted i.e., the model was trained iteratively on data of

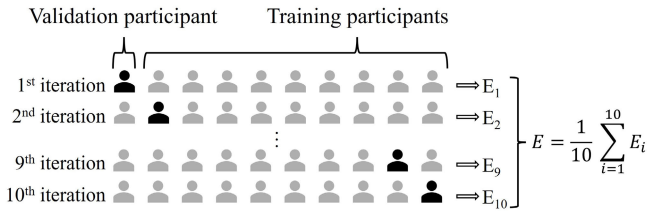


Fig. 4. Overview of the leave-one-participant-out cross-validation process with data of the construction set.

the training set and its performance validated on the participant of the validation set (Figure 4). This process was repeated until every participant was used in the validation set once. Therefore, given a combination of hyperparameters, ten models were trained. Optimal hyperparameters were chosen as the combinations that resulted in the lowest average percentages of missed and extra ICs.

3) *ICs Detection*: Once trained, the network returned the predicted IC likelihood for each instance, consisting of an array of size $1 \times N$. Likelihood peaks with a minimum likelihood of 0.04, a minimum prominence of 0.01, and a minimum interpeak distance of 0.2 s were regarded as detected ICs and used to segment strides in the WB. The threshold values were tuned via grid search. The i^{th} stride of a WB was defined as the time interval between the i^{th} and the $(i + 2)^{th}$ ICs. No distinction was made between left and right strides.

E. Step 2 – Gait Speed Estimator

Stride-by-stride gait speed is strongly related to stride length, typically estimated by double integration of the acceleration signals which is prone to high errors, especially in long recordings [56]. Drift errors can be partially mitigated by zero-velocity update [57] or biomechanical models [58], although these techniques are effective when the IMU is fixed on the foot. As an alternative, feature-based machine learning algorithms can be used to directly infer stride-by-stride gait speed from accelerometers and gyroscopes readings during previously segmented strides [20], [36], [59]. Gaussian process regression (GPR) has proved to be valid for estimating gait speed on a fixed-time window basis with data of an IMU on the lower-back [28] and head [21]. Unlike other machine learning algorithms, GPR does not assume a fixed functional form for the mapping between input features and output variables. This flexibility makes GPR well-suited for capturing complex, non-linear relationships, such as those between IMU features and gait speed.

In the present study, a similar algorithm is used to estimate gait speed from acceleration and angular velocity on a stride basis, by feeding it with features derived from the previously segmented strides. The algorithm was developed using Matlab.

1) *Preprocessing*: For each detected stride, the norms of triaxial acceleration and angular velocity were low-pass filtered. For each stride, 37 features including time-based statistics (e.g., mean, variance, duration, covariance, etc.) and frequency-based parameters (e.g., dominant frequencies, etc.) were calculated from acceleration and angular velocity, based on previous studies [28], [29], [36], [60], [61], [62].

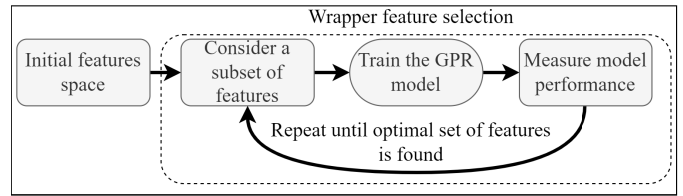


Fig. 5. Flow chart of the wrapper feature selection method based on the GPR model.

Additionally, height and weight were included in the initial feature space [60], for a total amount of 39 features. All the features were scaled using their construction set range.

2) Gaussian Process Regression:

a) *Model*: GPR models are a class of non-parametric kernel-based probabilistic models, allowing for non-linear relationships between variables and hence suitable for complex data analysis [63]. The properties of the Gaussian process used to fit the data are set by the covariance function - or kernel - and its hyperparameters - typically the length scale and the signal and noise standard deviations [64].

In the present study, a GPR model with a squared exponential kernel was used. The length scale (2.06), signal standard deviation (0.58), and the noise standard deviation (0.11) were optimized via random search.

b) *Feature selection*: To reduce the computational cost associated to a machine learning method, dimensionality reduction should always be pursued [37]. In this study, a forward wrapper feature selection method was employed (Fig. 5). This method aims to maximize the informative content of a predefined set of features without generating new ones. While this may overlook some lesser-known relevant features, it is particularly useful when prior knowledge identifies features likely to be most informative. Initially, features of the construction set were ranked based on their relevance using the Pearson correlation coefficients calculated between each feature and the target gait speed for all training subjects. Features with higher absolute Pearson correlation values were considered more relevant for predicting gait speed. Starting with an empty feature set, features were iteratively added to the GPR model, with the next most relevant feature added to the current feature subset in each iteration. To ensure robustness and prevent overfitting, for each candidate feature subset, the GPR model was trained using leave-one-subject-out cross-validation (Figure 4). The performance of each feature subset was evaluated based on the average Mean Absolute Error (MAE) of the predicted gait speed of the cross-validation folds. The feature subset of lowest dimensionality that resulted in an average MAE lower than 0.1 m/s was selected as the optimal set of features for the GPR model. The best features space included nine time-domain features derived only from acceleration (Table II).

F. External Validation and Statistical Analysis

A predicted IC was considered a true IC if it was the closest detected IC from a target IC and their temporal distance was lower than 0.2 s. Unmatched predicted and target ICs were considered extra and missed ICs, respectively. From the

TABLE II
FINAL FEATURES SPACE

| Feature | Formula |
|--|--|
| Stride duration (1 st) | l/f_s |
| Sum of absolute values (2 nd) | $\sum a_n $ |
| Relative step amplitude (3 rd) | $\frac{\max(a_n) - \min(a_n)}{l}$ |
| Range (4 th) | $\max(a_n) - \min(a_n)$ |
| Absolute step amplitude (5 th) | $\max(a_n) - \text{mean}(a_n)$ |
| Minimum (6 th) | $\min(a_n)$ |
| Variance (7 th) | $\frac{1}{l-1} \sum (a_n - \text{mean}(a_n))^2$ |
| Sum of squared values (8 th) | $\sum (a_n)^2$ |
| Mean of vertical velocity (9 th) | $\text{mean} \left(\int_{t_0}^{t_1} a_v dt \right)$ |

Features ranking is shown between parentheses. l : number of data points; f_s : sampling frequency; a_n : norm of acceleration; a_v : vertical acceleration.

numbers of true, missed, and extra ICs, sensitivity (2), positive predicted value (PPV) (3), and F1-score (4) were derived:

$$\text{Sensitivity} = \frac{\text{true ICs}}{\text{true ICs} + \text{missed ICs}} \quad (2)$$

$$\text{PPV} = \frac{\text{true ICs}}{\text{true ICs} + \text{extra ICs}} \quad (3)$$

$$\text{F1-score} = \frac{2 \times \text{PPV} \times \text{sensitivity}}{\text{PPV} + \text{sensitivity}} \quad (4)$$

For true ICs, the time agreement between predicted and target ICs was evaluated in terms of MAE, mean error (ME), SD and median absolute error (MDAE). For detected strides, agreement between predicted and target gait speed was evaluated in terms of MAE, ME, median error (MDE), error SD and correlation index. Normality of the distributions of gait speed values and errors was evaluated with the Anderson-Darling test [65], which resulted in the distributions not being normal ($p < 0.001$). Consistently, the Spearman correlation coefficient (ρ) was chosen to measure correlation. Agreement between the predicted and target gait speed values was also evaluated for both the Lab-Based and the Real-World test sets through error plots, where average values are plotted against their differences [66]. Additionally, to assess the robustness of the method in the estimation of gait speed across different walking conditions, a statistical comparison was performed between Lab-Based and Real-World absolute errors using bootstrapping with 10000 iterations at 95% confidence interval [67]. The gait speed errors of the Real-World test set were analysed to test whether gait speed or WB duration significantly affected the final error. Gait speed errors were grouped by target speed in slower (< 1 m/s), medium (1 m/s-1.5 m/s) and faster (> 1.5 m/s) speed regimes, according to [21]; and by WB duration in very short (< 10 s), short (10 s-30 s), medium (30 s-60 s) and long (> 60 s) WB durations, according to [9]. The three speed regime groups were graphically compared through boxplots. Boxplots whose notches did not overlap had different medians with 5% significance level [68]. The four WB duration groups were graphically compared through histograms, and statistically analysed with the non-parametric Kruskal-Wallis test, with 1% significance level adjusted post-hoc with the Bonferroni correction to account for multiple comparisons [69]. All statistical analyses were performed with Matlab and R 4.3.1.

TABLE III
RESULTS OBTAINED BY THE STRIDE DETECTOR

| | Real-World | | Lab-Based | |
|-----------------|------------|------|-----------|------|
| | TRS | TS | TRS | TS |
| Sensitivity (%) | 96.1 | 92.1 | 98.5 | 97.6 |
| PPV (%) | 95.1 | 93.3 | 95.2 | 93.9 |
| F1-score (%) | 95.6 | 92.7 | 96.8 | 95.7 |
| MAE (ms) | 10 | 30 | 10 | 20 |
| ME (ms) | 0 | 0 | 0 | 0 |
| SD (ms) | 20 | 30 | 10 | 10 |
| MDAE (ms) | 10 | 20 | 10 | 20 |

Results obtained by the stride detector with ICs of the Lab-Based and Real-World training set (TRS) and test set (TS).

TABLE IV
RESULTS OBTAINED BY THE GAIT SPEED ESTIMATOR

| | Real-World | | Lab-Based | |
|-----------|--------------|--------------|--------------|--------------|
| | TRS | TS | TRS | TS |
| MAE (m/s) | 0.076 (6.4%) | 0.081 (8.6%) | 0.084 (7.7%) | 0.081 (8.2%) |
| ME (m/s) | 0.000(-0.7%) | 0.019 (1.3%) | 0.036 (2.8%) | 0.028 (2.9%) |
| SD (m/s) | 0.065 | 0.066 | 0.067 | 0.059 |
| ρ | 0.86 | 0.91 | 0.87 | 0.87 |

Agreement between predicted and target gait speed values with data of the TRS and TS. Percentage values of MAE and ME are reported between parentheses. ρ : Spearman correlation coefficient.

III. RESULTS

Classification of ICs resulted in a F1-score close to 93% with the Real-World test set and 96% with the Lab-Based test set (Table III). True ICs were detected with a ME less than 10 ms for both conditions, with SD between 20 and 40 ms. The MDAE did not exceed 20 ms. Since the H-IMU sampled at 100 Hz (sampling interval = 10 ms), errors in ICs detection were rounded to tens of milliseconds. Overall, gait speed was estimated with a ME less than 0.04 m/s and a MAE around 0.08 m/s (Table IV). The Spearman correlation coefficient between target and predicted gait speed was over 0.87 for both the Lab-Based and Real-World test sets. For both conditions, the interquartile range (IQR) of errors were smaller than 0.13 m/s (Fig. 6). The bootstrapping analysis comparing the MAE between Lab-Based and Real-World conditions yielded a 95% confidence interval for ΔMAE of $[-0.0031, 0.0026]$, indicating no significant difference between the two conditions. The median errors on gait speed values in the Lab-Based and Real-World test sets were 0.08 m/s and 0.06 m/s for the slower speed regime, 0.03 m/s and 0.01 m/s for the medium speed regime, 0.06 m/s and -0.08 m/s for the faster speed regime (Fig. 7). For both test sets, medians in the three speed regimes showed significant differences, as their notch regions did not overlap. Gait speed errors of the Real-World test set were grouped by WB duration into four groups (Fig. 8). Very short, short, medium, and long WBs accounted for 38.5%, 32.4%, 15.4%, and 13.8% of WBs; and for 2.8%, 8.8%, 15.1%, and 73.3% of strides, respectively. The Kruskal-Wallis test for the multiple comparison between the four groups of WB duration resulted in a p -value greater than 0.01, thus accepting the null hypothesis of errors coming from the same distribution. The performance of the proposed method was directly compared to that of other established methods for ICs detection and/or gait speed estimation based on a single IMU. Table V included results reported by studies based on a

TABLE V
METHODS BASED ON A H-IMU FOR ESTIMATION OF ICs AND/OR GAIT SPEED OF HEALTHY PARTICIPANTS

| Study | Sensor positioning | Experimental procedure | ICs detection error | Gait speed estimation error |
|--------------------------|--------------------|--|---|--|
| Tasca | Head | Indoor straight and curvilinear walking at different speed regimes | Sensitivity: 97.6% ME: 0 ms MAE: 20 ms SD: 10 ms | ρ Spearman: 91% MAE: 0.08 m/s (8.2%) ME: 0.02 m/s (1.3%) SD: 0.059 m/s |
| Jarchi [70] | Ear | Indoor walking on treadmill at increasing inclines | ME: 17 ms SD: 22 ms | |
| Hwang [15] | Head | Outdoor walking around a 400 m track | ME: 14 ms SD: 14 ms | |
| Zihajezadeh [21] | Glasses | Indoor straight walking at different speed regimes | | ρ Pearson: 96% MAE: 6.5% SD: 3.1% |
| Tomc ^a [18] | Glasses | Indoor walking at different speed regimes | ME: 0.6% of gait cycle SD: 7.0% of gait cycle | |
| Seifer [19] | Hearing-aid | Indoor walking at different speed regimes | Sensitivity: 99.8% ME: 12 ms SD: 32 ms | |
| Seifer [20] | Hearing-aid | Indoor walking at different speed regimes | | MAE: 0.18 m/s SD: 0.14 |
| Decker ^b [22] | Hearing-aid | Indoor straight walking at different speed regimes. | Sensitivity: 99.7% ME: 3 ms | |
| Apostolopoulos [71] | Glasses | Indoor straight walking at normal speed in environment free of obstacles and people. | Error rate: 1.92% | |

Summary of the studies proposing methods for ICs detection and/or gait speed estimation with a single H-IMU. For the table content and color legend, see Table VI. ^aValues of ME and SD are expressed as percentage of the gait cycle during the fast walking trials, associated to the lowest reported error.

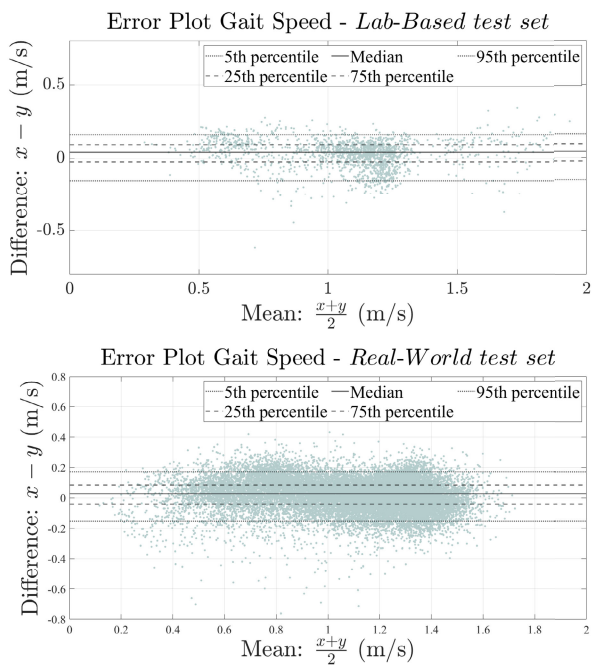


Fig. 6. Difference of predicted and target gait speed values against their mean. The 5th, 25th, 50th, 75th, and 95th percentiles were -0.152 , -0.023 , 0.043 , 0.091 and 0.162 m/s for the lab-based test set and -0.153 , -0.041 , 0.027 , 0.086 and 0.171 m/s for the real-world test set.

single head-worn inertial sensor. Studies reported in Table V presented methods that were validated under structured supervised settings; therefore, their results were compared to those obtained by the proposed method with the Lab-Based dataset, corresponding to similar experimental conditions. Table VI included methods based on a single IMU validated in unsupervised real-world conditions. Since no other studies based on H-IMU methods were validated in real-world settings, performance of the proposed method with the Real-World dataset

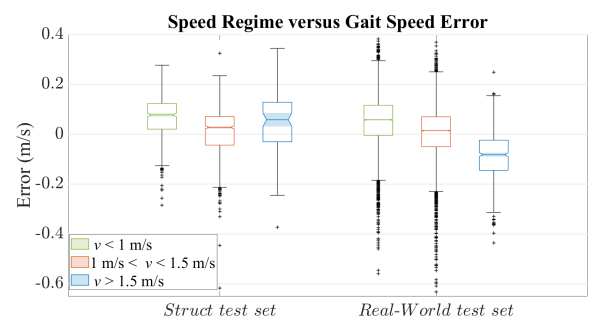


Fig. 7. Boxplots of the distribution of gait speed errors for the lab-based and real-world test sets at by speed regime. Black crosses represented outliers. Shaded areas represented the notches, corresponding to $MDE \pm (1.57 \times IQR) / \sqrt{n}$, where n was the number of observations.

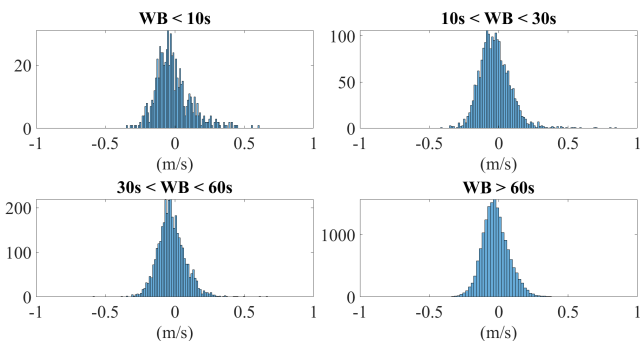


Fig. 8. Histograms of the distributions of gait speed errors for the Real-World test set grouped by WB duration. The number of bins was set to 100.

were compared to previous studies conducted in unsupervised real-world conditions based on different well-established IMU locations such as the lower back, wrist, and lower limbs (Table VI). Due to the different testing approaches adopted by each study, the reported performance metrics and their

TABLE VI

IMU-BASED METHODS VALIDATED IN REAL-WORLD CONDITIONS FOR ESTIMATION OF ICs AND/OR GAIT SPEED OF HEALTHY PARTICIPANTS

| Study | Sensor positioning | Experimental procedure | ICs detection error | Gait speed estimation error |
|--------------------------|--------------------|---|---|---|
| Tasca | Head | Unsupervised real-world settings (only level walking) | Sensitivity: 92.1% ME: 0 ms MAE: 30 ms SD: 30 ms | ρ Spearman: 91% MAE: 0.08 m/s (8.6%) ME: 0.02 m/s (1.3%) SD: 0.07 m/s |
| Ionescu [72] | Trunk | Simulations of daily life activities in clinical settings | | ME: 0.09 m/s SD: 0.15 m/s |
| Kirk [9] | Waist | Unsupervised real-world settings | | ICC: 0.88 ME: 0.04 m/s CI: -0.18–0.27 m/s |
| Micò-Amigo [10] | Waist | Unsupervised real-world settings | Sensitivity: 80% MAE: 60 ms CI: 50–60 ms | |
| Fasel [60] | Wrist | Supervised walking in urban and rural environment | | ρ Spearman: 71% MDAE: -0.01 m/s IQR: 0.18 m/s |
| Baroudi ^a [7] | Thigh | Unsupervised real-world settings | | CCC: 0.8 ME: 0.00 m/s SD: 0.05 m/s |
| Storm [73] | Shank | Unsupervised real-world settings (no stairs) | Sensitivity: 100% MAE: 14 ms SD: 8 ms | |
| Romijnders [8] | Both Feet | Unsupervised real-world settings | Sensitivity: 98% MDAE: 10 ms IQR: 20 ms | |

Summary of the studies proposing methods for ICs detection and/or gait speed estimation in real-world conditions. Colors of metrics refer to different performance aspects (*Orange*: classification error; *Blue*: error bias; *Green*: error variability; *Purple*: correlation with ground truth). ME: Mean error; MAE: Mean Absolute Error; MDAE: Median Absolute Error; SD: Standard Deviation of residuals; IQR: Inter-Quartiles Range of residuals; CI: Confidence Interval of residuals; CCC: Concordance Correlation Coefficient; ICC: Intra-Class Correlation coefficient; ρ Pearson: Pearson correlation coefficient; ρ Spearman: Spearman correlation coefficient. ^aSince the original paper did not report explicitly overall ME and SD, average values of ME and SD were calculated by the authors from Table 3 of the original paper for consistency to the results of the other reported studies.

dimensions are not consistent throughout the Tables and do not allow a direct comparison between the methods. However, at least one metric of bias and one of variability were reported. When available, sensitivity of ICs detection and metrics of correlation between predicted and target gait speed were reported as well. For studies involving both healthy and pathological participants, only results referring to healthy participants were included in the Tables, as the application of the proposed method to diseased gait goes beyond the goals of the study. For studies with multiple experimental conditions, either the results of the condition most similar to the present study or the aggregated results (when available) were considered.

IV. DISCUSSION

This study proposed and validated a machine learning method for stride-by-stride gait speed estimation from real world gait data of healthy subjects recorded by a head-worn IMU. To this end, participants were equipped with a IMU on their head (H-IMU), and with the INDIP system, including pressure insoles for both feet and magneto IMU for feet and lower-back. Data were recorded during a set of lab-based walking trials as well as 2.5-hours unsupervised real-world acquisitions, allowing to record a variety of activities of daily life in an ecologically valid environment. Data from the INDIP system were used to generate target timings of ICs and target gait speed, while acceleration and angular velocity recorded by the H-IMU were used as input to the method to i) detect ICs and use them to segment strides, and ii) estimate stride-by-stride gait speed. The overall accuracy of ICs detection on the training set, as quantified by the F1-score, was high (Lab-Based: $\approx 97\%$, Real-World: $\approx 96\%$), and the deep learning

model showed robust generalization skill on unseen data of the test set (Lab-Based: $\approx 96\%$, Real-World: $\approx 93\%$). The high values of sensitivity ($\approx 98\%$) and PPV ($\approx 94\%$) with the Lab-Based test set denoted the ability of the model to detect ICs with few missed and extra events. As expected, slight drops in PPV (93.3%) and sensitivity (92.1%) were observed with the Real-World test set due to the increased complexity of gait. Regarding gait speed, the proposed method resulted in small errors for all the analysed conditions (Lab-Based MDE: 0.027 m/s; Real-World MDE: 0.043 m/s), although a greater number of outliers was found in the Real-World test set (Fig. 6). Nevertheless, by assuming a clinically significant minimal change in gait speed between 0.1 and 0.2 m/s [74], the proposed method seems to be a promising solution for clinical applications. The walking environment did not seem to affect accuracy, as demonstrated by the results of the bootstrapping analysis on gait speed absolute errors across the two conditions (CI of Δ MAE between -0.0031 and 0.0026 m/s).

Statistically significant differences were found at different speed regimes (Fig. 7) suggesting that the method performance was affected by speed. Interestingly, the model resulted in lower errors with strides at speed between 1 m/s and 1.5 m/s (median error: 0.015 m/s), while the magnitude of errors increased at lower (median error: 0.058 m/s) and faster (median error: 0.082 m/s) speeds. A potential way to mitigate this effect would be to train separate models tailored to specific gait speed ranges [21]. On the other hand, gait speed errors resulted in similar distributions for the four groups of WB duration (Fig. 8). According to the Kruskal-Wallis test, no significant differences were found between error distributions of groups of WB duration i.e.,

the method performance was not affected by the duration of the processed WB. Surprisingly, the most effective features for the GPR model were derived uniquely from acceleration data, suggesting that, in the experimental conditions of this study, rotational movements played a less critical role than linear movements in determining gait speed. This allows gait speed to be estimated without the need to collect data from the gyroscope, reducing power consumption, which is a crucial aspect for wearable systems. Conversely from previous studies utilizing a head-worn IMU for gait analysis, this paper validated the new proposed approach in unsupervised conditions and without adopting a structured gait protocol. This is a significant step forward, given that the motion of the head when moving in daily context is predominantly nondeterministic and largely affected by contextual factors and the environment. In structured gait protocols, participants usually walk facing the direction of progression without encountering external stimuli, resulting in minimal head movements and rotations. In contrast, real-world conditions involve a variety of external stimuli and interactions, causing the head to move and rotate in response [75]. This leads to more complex and variable inertial signals recorded at the head level. The limitations of structured gait protocols in capturing these real-world behaviors highlight the necessity for robust algorithm development tailored to the unique challenges of head-worn sensors, especially for accurate gait analysis in everyday environments. The performance of ICs detection in the lab-based environment was comparable or better than those of previous studies using H-IMU - with only [19] and [22] achieving a slightly higher sensitivity. For gait speed estimation, the proposed method matched the performance of previous methods, with only [21] reporting slightly better values of correlation coefficient and relative MAE (Table V). As expected, methods based on IMU worn on the lower limbs [8], [73] resulted in higher sensitivity in real-world conditions (Table VI). Focusing on true ICs, the proposed method resulted in time errors in the same range of previous studies. Surprisingly, errors of the gait speed estimator with the Real-World test set (MAE: 0.02 m/s) were similar to those reported by Kirk et al. [9] and Ionescu et al. [72], despite using a sensor mounted on the head instead of the lower back. However, while the present study considered only gait data during level walking, the above-mentioned studies included inclined walking as well (climbing stairs or ramps); therefore, caution may be exercised when comparing the methods. Among other methods validated in real-world conditions, the best performance was achieved by the work of Baroudi et al. [7], proposing subject-specific models to estimate gait speed. This was not surprising, as the use of a thigh-worn IMU is expected to result in more robust gait speed estimates with respect to a H-IMU.

The head is a promising site for wearable sensors due to its usability, with devices like glasses, earbuds, and hearing aids being widely used and easily standardized for placement, even by non-experts [24], [71]. However, gait-related oscillations are dampened at the head to preserve the proper functioning of the vestibular and proprioceptive systems [71], [76], and non-gait-related movements introduce confounding factors,

requiring robust algorithms to accurately interpret data in real-world environments.

One limitation of the present study is that only data from WBs detected by the INDIP was used. This means that the correct identification of gait sequences influenced the detection of ICs [77]. However, methods for reliably detecting gait from data of head-mounted sensors were previously reported [78], [79]. Another limitation is that the method was trained on level walking only and therefore, results cannot be generalized for activities including climbing stairs in buildings or walking on ramps. The experiments conducted as part of this study aimed at evaluating the general applicability of the proposed method to gait analysis in real-world conditions; therefore, the effect of potential confounding factors such as turns, stops and walking on challenging terrains, was not specifically analysed. Future studies are needed to address these limitations and assess the generalization skills and the clinical applicability of the proposed method to subjects with different gait patterns and diseases causing motor impairments.

The proposed method demonstrated accuracy in real-world conditions comparable to structured settings, suggesting its potential for applications such as telemonitoring, telerehabilitation, and clinical trials, where naturalistic data can provide valuable insights into the efficacy of drugs or interventions. It may also support large-scale studies of population health and mobility, aiding in the development of targeted interventions and mobility aids. These findings emphasize the importance of validating gait analysis methods in real-world environments to bridge the gap between controlled experiments and practical use.

V. CONCLUSION

This paper presented a method that accurately and robustly detected initial foot-to-ground contacts and stride-by-stride gait speed from a head mounted inertial sensor, even in the presence of the confounding factors typical of real-world gait, and also in previously unseen data. The error committed by the proposed method was found to be affected by the speed regime but not by the duration of the walking bouts, suggesting that the method maintains consistent accuracy over varying walking bout durations but may require further tuning for different walking speeds. The proposed method matched the performance of other algorithms based on sensors placed on the lower limbs, wrist, or pelvis in similar populations. The use of a single head-mounted IMU may be helpful in long-term gait studies in ecological conditions, with head-worn instrumented devices such as hearing aids or smart glasses, being already integrated in the daily life of young and elderly people. In conclusion, the proposed method opens the door to further exploitation of new technologies embedded in smart head-worn devices for digital mobility assessment.

REFERENCES

- [1] S. Fritz and M. Lusardi, "White paper: "Walking speed: The sixth vital sign,"" *J. Geriatric Phys. Therapy*, vol. 32, no. 2, pp. 2–5, 2009, doi: [10.1519/00139143-200932020-00002](https://doi.org/10.1519/00139143-200932020-00002).
- [2] A. Polhemus et al., "Walking on common ground: A cross-disciplinary scoping review on the clinical utility of digital mobility outcomes," *npj Digit. Med.*, vol. 4, no. 1, Oct. 2021, Art. no. 149, doi: [10.1038/s41746-021-00513-5](https://doi.org/10.1038/s41746-021-00513-5).

- [3] I. Galperin et al., "Associations between daily-living physical activity and laboratory-based assessments of motor severity in patients with falls and Parkinson's disease," *Parkinsonism Rel. Disorders*, vol. 62, pp. 85–90, May 2019, doi: [10.1016/j.parkreldis.2019.01.022](https://doi.org/10.1016/j.parkreldis.2019.01.022).
- [4] F. Kluge et al., "Real-world gait detection using a wrist-worn inertial sensor: Validation study," *JMIR Formative Res.*, vol. 8, May 2024, Art. no. e50035, doi: [10.2196/50035](https://doi.org/10.2196/50035).
- [5] A. Soltani, H. Dejnabadi, M. Savary, and K. Aminian, "Real-world gait speed estimation using wrist sensor: A personalized approach," *IEEE J. Biomed. Health Informat.*, vol. 24, no. 3, pp. 658–668, Mar. 2020, doi: [10.1109/JBHI.2019.2914940](https://doi.org/10.1109/JBHI.2019.2914940).
- [6] M. Zanoletti et al., "Combining different wearable devices to assess gait speed in real-world settings," *Sensors*, vol. 24, no. 10, p. 3205, May 2024, doi: [10.3390/s24103205](https://doi.org/10.3390/s24103205).
- [7] L. Baroudi, M. W. Newman, E. A. Jackson, K. Barton, K. A. Shorter, and S. M. Cain, "Estimating walking speed in the wild," *Frontiers Sports Act. Living*, vol. 2, Nov. 2020, Art. no. 583848, doi: [10.3389/fspor.2020.583848](https://doi.org/10.3389/fspor.2020.583848).
- [8] R. Romijnders et al., "Ecological validity of a deep learning algorithm to detect gait events from real-life walking bouts in mobility-limiting diseases," *Frontiers Neurol.*, vol. 14, Oct. 2023, Art. no. 1247532, doi: [10.3389/fneur.2023.1247532](https://doi.org/10.3389/fneur.2023.1247532).
- [9] C. Kirk et al., "Mobilise-D insights to estimate real-world walking speed in multiple conditions with a wearable device," *Sci. Rep.*, vol. 14, p. 1754, Jan. 2024. [Online]. Available: <https://doi.org/10.1038/s41598-024-51766-5>
- [10] M. E. Micó-Amigo et al., "Assessing real-world gait with digital technology? Validation, insights and recommendations from the Mobilise-D consortium," *J. NeuroEng. Rehabil.*, vol. 20, no. 1, p. 78, Jun. 2023, doi: [10.1186/s12984-023-01198-5](https://doi.org/10.1186/s12984-023-01198-5).
- [11] C. Mazzà et al., "Technical validation of real-world monitoring of gait: A multicentric observational study," *BMJ Open*, vol. 11, no. 12, Dec. 2021, Art. no. e050785, doi: [10.1136/bmjopen-2021-050785](https://doi.org/10.1136/bmjopen-2021-050785).
- [12] A. Cristiano, A. Sanna, and D. Trojaniello, "Validity of a smart-glasses-based step-count measure during simulated free-living conditions," *Information*, vol. 11, no. 9, p. 404, Aug. 2020, doi: [10.3390/info11090404](https://doi.org/10.3390/info11090404).
- [13] N. Biswas, S. Chakrabarti, L. D. Jones, and S. Ashili, "Smart wearables addressing gait disorders: A review," *Mater. Today Commun.*, vol. 35, Jun. 2023, Art. no. 106250, doi: [10.1016/j.mtcomm.2023.106250](https://doi.org/10.1016/j.mtcomm.2023.106250).
- [14] C. K. Jung, J. Kim, and H. C. Rhim, "Validation of an ear-worn wearable gait analysis device," *Sensors*, vol. 23, no. 3, p. 1244, Jan. 2023, doi: [10.3390/s23031244](https://doi.org/10.3390/s23031244).
- [15] T.-H. Hwang, J. Reh, A. O. Effenberg, and H. Blume, "Real-time gait analysis using a single head-worn inertial measurement unit," *IEEE Trans. Consum. Electron.*, vol. 64, no. 2, pp. 240–248, May 2018, doi: [10.1109/TCE.2018.2843289](https://doi.org/10.1109/TCE.2018.2843289).
- [16] P. Caserman, P. Krabbe, J. Wojtusich, and O. von Stryk, "Real-time step detection using the integrated sensors of a head-mounted display," in *Proc. IEEE Int. Conf. Syst., Man, Cybern. (SMC)*, Oct. 2016, pp. 3510–3515, doi: [10.1109/SMC.2016.7844777](https://doi.org/10.1109/SMC.2016.7844777).
- [17] J. Hellec, F. Chorin, A. Castagnetti, O. Guérin, and S. S. Colson, "Smart eyeglasses: A valid and reliable device to assess spatiotemporal parameters during gait," *Sensors*, vol. 22, no. 3, p. 1196, Feb. 2022, doi: [10.3390/s22031196](https://doi.org/10.3390/s22031196).
- [18] M. Tomc and Z. Matjačić, "Real-time gait event detection with adaptive frequency oscillators from a single head-mounted IMU," *Sensors*, vol. 23, no. 12, p. 5500, Jun. 2023, doi: [10.3390/s23125500](https://doi.org/10.3390/s23125500).
- [19] A.-K. Seifer, E. Dorschky, A. Küderle, H. Moradi, R. Hannemann, and B. M. Eskofier, "EarGait: Estimation of temporal gait parameters from hearing aid integrated inertial sensors," *Sensors*, vol. 23, no. 14, p. 6565, Jul. 2023, doi: [10.3390/s23146565](https://doi.org/10.3390/s23146565).
- [20] A.-K. Seifer, A. Küderle, E. Dorschky, H. Moradi, R. Hannemann, and B. M. Eskofier, "Step length and gait speed estimation using a hearing aid integrated accelerometer: A comparison of different algorithms," *IEEE J. Biomed. Health Informat.*, vol. 28, no. 11, pp. 6619–6628, Nov. 2024.
- [21] S. Zihajezadeh and E. J. Park, "A Gaussian process regression model for walking speed estimation using a head-worn IMU," in *Proc. 39th Annu. Int. Conf. IEEE Eng. Med. Biol. Soc. (EMBC)*, Jul. 2017, pp. 2345–2348, doi: [10.1109/EMBC.2017.8037326](https://doi.org/10.1109/EMBC.2017.8037326).
- [22] J. Decker, L. Boborzi, R. Schniepp, K. Jahn, and M. Wuehr, "Mobile spatiotemporal gait segmentation using an ear-worn motion sensor and deep learning," *Sensors*, vol. 24, no. 19, p. 6442, Oct. 2024, doi: [10.3390/s24196442](https://doi.org/10.3390/s24196442).
- [23] J. R. Fang, R. Pahwa, K. E. Lyons, T. Zanotto, and J. J. Sosnoff, "Examining the validity of smart glasses in measuring spatiotemporal parameters of gait among people with Parkinson's disease," *Gait Posture*, vol. 113, pp. 139–144, Sep. 2024, doi: [10.1016/j.gaitpost.2024.06.001](https://doi.org/10.1016/j.gaitpost.2024.06.001).
- [24] I. Kiprijanovska et al., "Smart glasses for gait analysis of Parkinson's disease patients," in *Proc. 46th MIPRO ICT Electron. Conv. (MIPRO)*, May 2023, pp. 385–390, doi: [10.23919/MIPRO57284.2023.10159926](https://doi.org/10.23919/MIPRO57284.2023.10159926).
- [25] D. J. Geerse, B. Coolen, and M. Roerdink, "Quantifying spatiotemporal gait parameters with HoloLens in healthy adults and people with Parkinson's disease: Test-retest reliability, concurrent validity, and face validity," *Sensors*, vol. 20, no. 11, p. 3216, Jun. 2020, doi: [10.3390/s20113216](https://doi.org/10.3390/s20113216).
- [26] Y. Diao, Y. Ma, D. Xu, W. Chen, and Y. Wang, "A novel gait parameter estimation method for healthy adults and postoperative patients with an ear-worn sensor," *Physiol. Meas.*, vol. 41, no. 5, Jun. 2020, Art. no. 05NT01, doi: [10.1088/1361-6579/ab87b5](https://doi.org/10.1088/1361-6579/ab87b5).
- [27] E. Giannouli, O. Bock, S. Mellone, and W. Zijlstra, "Mobility in old age: Capacity is not performance," *BioMed Res. Int.*, vol. 2016, no. 1, 2016, Art. no. 3261567, doi: [10.1155/2016/3261567](https://doi.org/10.1155/2016/3261567).
- [28] S. Zihajezadeh and E. J. Park, "Regression model-based walking speed estimation using wrist-worn inertial sensor," *PLoS ONE*, vol. 11, no. 10, Oct. 2016, Art. no. e0165211, doi: [10.1371/journal.pone.0165211](https://doi.org/10.1371/journal.pone.0165211).
- [29] H. Vathsangam, A. Emken, D. Spruijt-Metz, and G. S. Sukhatme, "Toward free-living walking speed estimation using Gaussian process-based regression with on-body accelerometers and gyroscopes," in *Proc. 4th Int. Conf. Pervasive Comput. Technol. Healthcare*, Mar. 2010, pp. 1–8, doi: [10.4108/ICST.PERVASIVEHEALTH2010.8786](https://doi.org/10.4108/ICST.PERVASIVEHEALTH2010.8786).
- [30] Y. Mao, T. Ogata, H. Ora, N. Tanaka, and Y. Miyake, "Estimation of stride-by-stride spatial gait parameters using inertial measurement unit attached to the shank with inverted pendulum model," *Sci. Rep.*, vol. 11, no. 1, Jan. 2021, Art. no. 1391, doi: [10.1038/s41598-021-81009-w](https://doi.org/10.1038/s41598-021-81009-w).
- [31] K. Seo, "Real-time estimation of walking speed and stride length using an IMU embedded in a robotic hip exoskeleton," in *Proc. IEEE Int. Conf. Robot. Autom. (ICRA)*, May 2023, pp. 12665–12671, doi: [10.1109/ICRA48891.2023.10160770](https://doi.org/10.1109/ICRA48891.2023.10160770).
- [32] D. A. Revi, S. M. M. De Rossi, C. J. Walsh, and L. N. Awad, "Estimation of walking speed and its spatiotemporal determinants using a single inertial sensor Worn on the thigh: From healthy to hemiparetic walking," *Sensors*, vol. 21, no. 21, p. 6976, Oct. 2021, doi: [10.3390/s21216976](https://doi.org/10.3390/s21216976).
- [33] A. Soltani et al., "Algorithms for walking speed estimation using a lower-back-worn inertial sensor: A cross-validation on speed ranges," *IEEE Trans. Neural Syst. Rehabil. Eng.*, vol. 29, pp. 1955–1964, 2021, doi: [10.1109/TNSRE.2021.3111681](https://doi.org/10.1109/TNSRE.2021.3111681).
- [34] D. Trojaniello et al., "Estimation of step-by-step spatio-temporal parameters of normal and impaired gait using shank-mounted magneto-inertial sensors: Application to elderly, hemiparetic, parkinsonian and choreic gait," *J. NeuroEng. Rehabil.*, vol. 11, no. 1, p. 152, 2014, doi: [10.1186/1743-0003-11-152](https://doi.org/10.1186/1743-0003-11-152).
- [35] W. Zijlstra and A. L. Hof, "Assessment of spatio-temporal gait parameters from trunk accelerations during human walking," *Gait Posture*, vol. 18, no. 2, pp. 1–10, Oct. 2003, doi: [10.1016/s0966-6362\(02\)00190-x](https://doi.org/10.1016/s0966-6362(02)00190-x).
- [36] M. Schimpl, C. Lederer, and M. Daumer, "Development and validation of a new method to measure walking speed in free-living environments using the Actibelt® platform," *PLoS ONE*, vol. 6, no. 8, Aug. 2011, Art. no. e23080, doi: [10.1371/journal.pone.0023080](https://doi.org/10.1371/journal.pone.0023080).
- [37] P. Khera and N. Kumar, "Role of machine learning in gait analysis: A review," *J. Med. Eng. Technol.*, vol. 44, no. 8, pp. 441–467, Nov. 2020, doi: [10.1080/03091902.2020.1822940](https://doi.org/10.1080/03091902.2020.1822940).
- [38] F. Salis et al., "A multi-sensor wearable system for the assessment of diseased gait in real-world conditions," *Frontiers Bioeng. Biotechnol.*, vol. 11, Apr. 2023, Art. no. 1143248, doi: [10.3389/fbioe.2023.1143248](https://doi.org/10.3389/fbioe.2023.1143248).
- [39] R. Romijnders, E. Warmerdam, C. Hansen, G. Schmidt, and W. Maetzler, "A deep learning approach for gait event detection from a single shank-worn IMU: Validation in healthy and neurological cohorts," *Sensors*, vol. 22, no. 10, p. 3859, May 2022, doi: [10.3390/s22103859](https://doi.org/10.3390/s22103859).
- [40] S. Ionut-Cristian and D. Dan-Marius, "Using inertial sensors to determine head motion—A review," *J. Imag.*, vol. 7, no. 12, p. 265, Dec. 2021, doi: [10.3390/jimaging7120265](https://doi.org/10.3390/jimaging7120265).
- [41] D. Kroneberg et al., "Less is more—Estimation of the number of strides required to assess gait variability in spatially confined settings," *Frontiers Aging Neurosci.*, vol. 10, Jan. 2019, Art. no. 435, doi: [10.3389/fnagi.2018.00435](https://doi.org/10.3389/fnagi.2018.00435).

- [42] L. Kribus-Shmiel, G. Zeilig, B. Sokolovski, and M. Plotnik, "How many strides are required for a reliable estimation of temporal gait parameters? Implementation of a new algorithm on the phase coordination index," *PLoS ONE*, vol. 13, no. 2, Feb. 2018, Art. no. e0192049, doi: [10.1371/journal.pone.0192049](https://doi.org/10.1371/journal.pone.0192049).
- [43] R. Cromwell, J. Schurter, S. Shelton, and S. Vora, "Head stabilization strategies in the sagittal plane during locomotor tasks," *Physiotherapy Res. Int.*, vol. 9, no. 1, pp. 33–42, Mar. 2004, doi: [10.1002/pri.298](https://doi.org/10.1002/pri.298).
- [44] T. Pozzo, A. Berthoz, and L. Lefort, "Head stabilization during various locomotor tasks in humans," *Exp. Brain Res.*, vol. 82, no. 1, pp. 97–106, Aug. 1990, doi: [10.1007/bf00230842](https://doi.org/10.1007/bf00230842).
- [45] A. Mannini and A. M. Sabatini, "A hidden Markov model-based technique for gait segmentation using a foot-mounted gyroscope," in *Proc. Annu. Int. Conf. IEEE Eng. Med. Biol. Soc.*, Aug. 2011, pp. 4369–4373, doi: [10.1109/IEMBS.2011.6091084](https://doi.org/10.1109/IEMBS.2011.6091084).
- [46] J. Wu et al., "Real-time gait phase detection on wearable devices for real-world free-living gait," *IEEE J. Biomed. Health Informat.*, vol. 27, no. 3, pp. 1295–1306, Mar. 2023, doi: [10.1109/JBHI.2022.3228329](https://doi.org/10.1109/JBHI.2022.3228329).
- [47] M. Zago et al., "Machine-learning based determination of gait events from foot-mounted inertial units," *Sensors*, vol. 21, no. 3, p. 839, Jan. 2021, doi: [10.3390/s21030839](https://doi.org/10.3390/s21030839).
- [48] H. Zhao et al., "Adaptive gait detection based on foot-mounted inertial sensors and multi-sensor fusion," *Inf. Fusion*, vol. 52, pp. 157–166, Dec. 2019, doi: [10.1016/j.inffus.2019.03.002](https://doi.org/10.1016/j.inffus.2019.03.002).
- [49] P. Rmy. (2020). *Temporal Convolutional Networks for Keras*. [Online]. Available: <https://github.com/philipperemy/keras-tcn>
- [50] E. Shelhamer, J. Long, and T. Darrell, "Fully convolutional networks for semantic segmentation," *IEEE Trans. Pattern Anal. Mach. Intell.*, vol. 39, no. 4, pp. 640–651, Apr. 2017, doi: [10.1109/TPAMI.2016.2572683](https://doi.org/10.1109/TPAMI.2016.2572683).
- [51] S. Bai, J. Z. Kolter, and V. Koltun, "An empirical evaluation of generic convolutional and recurrent networks for sequence modeling," 2018, *arXiv:1803.01271*.
- [52] F. Yu and V. Koltun, "Multi-scale context aggregation by dilated convolutions," 2015, *arXiv:1511.07122*.
- [53] S. Ioffe and C. Szegedy, "Batch normalization: Accelerating deep network training by reducing internal covariate shift," 2015, *arXiv:1502.03167*.
- [54] N. Srivastava, G. Hinton, A. Krizhevsky, I. Sutskever, and R. Salakhutdinov, "Dropout: A simple way to prevent neural networks from overfitting," *J. Mach. Learn. Res.*, vol. 15, no. 1, pp. 1929–1958, 2014. [Online]. Available: <http://jmlr.org/papers/v15/srivastava14a.html>
- [55] M. Shafiq and Z. Gu, "Deep residual learning for image recognition: A survey," *Appl. Sci.*, vol. 12, no. 18, p. 8972, Sep. 2022, doi: [10.3390/app12188972](https://doi.org/10.3390/app12188972).
- [56] Y. K. Thong, M. S. Woolfson, J. A. Crowe, B. R. Hayes-Gill, and D. A. Jones, "Numerical double integration of acceleration measurements in noise," *Measurement, J. Int. Meas. Confederation*, vol. 36, no. 1, pp. 73–92, Jul. 2004, doi: [10.1016/j.measurement.2004.04.005](https://doi.org/10.1016/j.measurement.2004.04.005).
- [57] Z. Wang and R. Ji, "Estimate spatial-temporal parameters of human gait using inertial sensors," in *Proc. IEEE Int. Conf. Cyber Technol. Autom., Control, Intell. Syst. (CYBER)*, Jun. 2015, pp. 1883–1888, doi: [10.1109/CYBER.2015.7288234](https://doi.org/10.1109/CYBER.2015.7288234).
- [58] W. Zijlstra, "Assessment of spatio-temporal parameters during unconstrained walking," *Eur. J. Appl. Physiol.*, vol. 92, nos. 1–2, pp. 39–44, Jun. 2004, doi: [10.1007/s00421-004-1041-5](https://doi.org/10.1007/s00421-004-1041-5).
- [59] A. Mannini and A. M. Sabatini, "Walking speed estimation using foot-mounted inertial sensors: Comparing machine learning and strap-down integration methods," *Med. Eng. Phys.*, vol. 36, no. 10, pp. 1312–1321, Oct. 2014, doi: [10.1016/j.medengphys.2014.07.022](https://doi.org/10.1016/j.medengphys.2014.07.022).
- [60] B. Fasel et al., "A wrist sensor and algorithm to determine instantaneous walking cadence and speed in daily life walking," *Med. Biol. Eng. Comput.*, vol. 55, no. 10, pp. 1773–1785, Oct. 2017, doi: [10.1007/s11517-017-1621-2](https://doi.org/10.1007/s11517-017-1621-2).
- [61] A. Atrsaei, F. Dadashi, B. Mariani, R. Gonzenbach, and K. Aminian, "Toward a remote assessment of walking foot and speed: Application in patients with multiple sclerosis," *IEEE J. Biomed. Health Informat.*, vol. 25, no. 11, pp. 4217–4228, Nov. 2021, doi: [10.1109/JBHI.2021.3076707](https://doi.org/10.1109/JBHI.2021.3076707).
- [62] S. Byun, H. J. Lee, J. W. Han, J. S. Kim, E. Choi, and K. W. Kim, "Walking-speed estimation using a single inertial measurement unit for the older adults," *PLoS ONE*, vol. 14, no. 12, Dec. 2019, Art. no. e0227075, doi: [10.1371/journal.pone.0227075](https://doi.org/10.1371/journal.pone.0227075).
- [63] C. E. Rasmussen, "Gaussian processes in machine learning," in *Advanced Lectures on Machine Learning* (Lecture Notes in Computer Science: Lecture Notes in Artificial Intelligence and Lecture Notes in Bioinformatics), vol. 3176. Berlin, Germany: Springer, 2004, pp. 63–71, doi: [10.1007/978-3-540-28650-9_4](https://doi.org/10.1007/978-3-540-28650-9_4).
- [64] A. Zhang, Z. C. Lipton, M. Li, and A. J. Smola, *Dive into Deep Learning*. Cambridge Univ. Press, 2023. [Online]. Available: <https://D2L.ai>
- [65] A. Ghasemi and S. Zahediasl, "Normality tests for statistical analysis: A guide for non-statisticians," *Int. J. Endocrinol. Metabolism*, vol. 10, no. 2, pp. 486–489, Dec. 2012, doi: [10.5812/ijem.3505](https://doi.org/10.5812/ijem.3505).
- [66] J. M. Bland and D. Altman, "Statistical methods for assessing agreement between two methods of clinical measurement," *Lancet*, vol. 327, no. 8476, pp. 307–310, Feb. 1986, doi: [10.1016/S0140-6736\(86\)90837-8](https://doi.org/10.1016/S0140-6736(86)90837-8).
- [67] P. I. Good, *Resampling Methods: A Practical Guide to Data Analysis*. Cham, Switzerland: Springer, 2006, doi: [10.1007/978-1-4757-3049-4](https://doi.org/10.1007/978-1-4757-3049-4).
- [68] R. Mcgill, J. W. Tukey, and W. A. Larsen, "Variations of box plots," *Amer. Statistician*, vol. 32, no. 1, pp. 12–16, Feb. 1978, doi: [10.1080/00031305.1978.10479236](https://doi.org/10.1080/00031305.1978.10479236).
- [69] Y. Hochberg and A. C. Tamhane, *Multiple Comparison Procedures*. Hoboken, NJ, USA: Wiley, 1987, doi: [10.1002/9780470316672](https://doi.org/10.1002/9780470316672).
- [70] D. Jarchi, C. Wong, R. M. Kwasnicki, B. Heller, G. A. Tew, and G.-Z. Yang, "Gait parameter estimation from a miniaturized ear-worn sensor using singular spectrum analysis and longest common subsequence," *IEEE Trans. Biomed. Eng.*, vol. 61, no. 4, pp. 1261–1273, Apr. 2014, doi: [10.1109/TBME.2014.2299772](https://doi.org/10.1109/TBME.2014.2299772).
- [71] I. Apostolopoulos, D. S. Coming, and E. Folmer, "Accuracy of pedometry on a head-mounted display," in *Proc. 33rd Annu. ACM Conf. Human Factors Comput. Syst.*, Apr. 2015, pp. 2153–2156, doi: [10.1145/2702123.2702143](https://doi.org/10.1145/2702123.2702143).
- [72] A. Paraschiv-Ionescu, A. Soltani, and K. Aminian, "Real-world speed estimation using single trunk IMU: Methodological challenges for impaired gait patterns," in *Proc. 42nd Annu. Int. Conf. IEEE Eng. Med. Biol. Soc. (EMBC)*, Jul. 2020, pp. 4596–4599, doi: [10.1109/EMBC44109.2020.9176281](https://doi.org/10.1109/EMBC44109.2020.9176281).
- [73] F. A. Storm, C. J. Buckley, and C. Mazzà, "Gait event detection in laboratory and real life settings: Accuracy of ankle and Waist sensor based methods," *Gait Posture*, vol. 50, pp. 42–46, Oct. 2016, doi: [10.1016/j.gaitpost.2016.08.012](https://doi.org/10.1016/j.gaitpost.2016.08.012).
- [74] R. W. Bohannon and S. S. Glenney, "Minimal clinically important difference for change in comfortable gait speed of adults with pathology: A systematic review," *J. Eval. Clin. Pract.*, vol. 20, no. 4, pp. 295–300, Aug. 2014, doi: [10.1111/jep.12158](https://doi.org/10.1111/jep.12158).
- [75] J. Windau and L. Itti, "Walking compass with head-mounted IMU sensor," in *Proc. IEEE Int. Conf. Robot. Autom. (ICRA)*, May 2016, pp. 5542–5547, doi: [10.1109/ICRA.2016.7487770](https://doi.org/10.1109/ICRA.2016.7487770).
- [76] C. Mazzà, M. Iosa, F. Pecoraro, and A. Cappozzo, "Control of the upper body accelerations in young and elderly women during level walking," *J. NeuroEng. Rehabil.*, vol. 5, no. 1, pp. 1–10, Dec. 2008, doi: [10.1186/1743-0003-5-30](https://doi.org/10.1186/1743-0003-5-30).
- [77] N. Roth et al., "Hidden Markov model based stride segmentation on unsupervised free-living gait data in Parkinson's disease patients," *J. NeuroEng. Rehabil.*, vol. 18, no. 1, p. 93, Dec. 2021, doi: [10.1186/s12984-021-00883-7](https://doi.org/10.1186/s12984-021-00883-7).
- [78] C. P. Burgos et al., "In-ear accelerometer-based sensor for gait classification," *IEEE Sensors J.*, vol. 20, no. 21, pp. 12895–12902, Nov. 2020, doi: [10.1109/JSEN.2020.3002589](https://doi.org/10.1109/JSEN.2020.3002589).
- [79] D. Loh, T. J. Lee, S. Zihajehzadeh, R. Hoskinson, and E. J. Park, "Fitness activity classification by using multiclass support vector machines on head-worn sensors," in *Proc. 37th Annu. Int. Conf. IEEE Eng. Med. Biol. Soc. (EMBC)*, Aug. 2015, pp. 502–505, doi: [10.1109/EMBC.2015.7318409](https://doi.org/10.1109/EMBC.2015.7318409).